Chapter 3

Oscillatory MHD Couette flow in a rotating system*

3.1 Introduction

The study of fluid flow in a rotating environment has considerable bearing on the problems of geophysical, astrophysical and fluid engineering applications. An extensive literature exists on the flow of fluids in a rotating frame. Nanda and Mohanty [206] have studied the hydromagnetic steady flow in a rotating channel with constant pressure gradient. Majumder [207] has studied the effect of wall conductances on the hydromagnetic flow in a rotating system. Datta and Jana [62] have discussed the effect of rotation and Hall current on the hydromagnetic flow using non-conducting walls. Jana et al. [208] have studied the MHD Couette flow in a rotating frame of reference when the fixed plate of the channel was a perfect conductor, the moving one was non-conducting . Nagy and Demendy [209] have studied the hydromagnetic flow under general wall conditions. The combined effects of Hall current and rotation on the flow structure and heat transfer in a generalised hydromagnetic flow have been studied by Nagy and Demendy [210]. Guria et al. [211] have studied the hydromagnetic flow in a rotating channel in the presence of inclined magnetic field. The unsteady Couette flow in a rotating system have been studied by Guria et al. [212]. The unsteady hydromagnetic

Published in **International Journal of Fluid Mechanics Research, 37(3)(2010), pp.251-266.**

Couette flow in a rotating system under boundary layer approximation has been studied by Mazumder [23], Ganapaty [213] and Guria et al. [214]. Hall effects on hydromagnetic rotating Couette flow has been analyzed by Das et al. [215]. Seth et al. [216] have considered hydromagnetic oscillatory Couette flow in rotating system with induced magnetic field. Transient hydromagnetic reactive Couette flow and heat transfer characteristic has been described by Das et al. [217] in a rotating frame of reference. An analysis of unsteady MHD Couette flow and heat transfer has been made by Gupta and Jain [218] taking rotating horizontal channel with suction/injection. Rajesh et al. [219] have derived an exact solution of oscillatory Ekman boundary layer flow through a porous medium bounded by two horizontal flat plates where one of the plates is at rest and the other one is oscillating in its own plane.

The present chapter is devoted to study the hydromagnetic Couette flow through a horizontal channel when one of the plate is oscillating about the mean velocity and the other is held at rest in a rotating system under boundary layer approximations. It is found that the unsteady part of the primary velocity increases while that part of the secondary velocity decreases with an increase in Hartmann number M. It is also found that phase of the shear stress due to unsteady part of the primary flow at the plate $\eta = 0$ has always a phase lead for $2K^2 < \omega$ and a phase lag for $2K^2 > \omega$. On the other hand, phase of the shear stress due to the unsteady part of the secondary flow has a phase lead over the plate oscillations.

3.2 Mathematical formulation and its solution

Consider the unsteady viscous incompressible electrically conducting fluid bounded by two infinitely long horizontal parallel plates separated by a distance d, the lower plate is held at rest and the upper plate is oscillating in its own plane with a velocity $U(t)$ about a constant mean velocity U_0 in the direction of x-axis where x-axis is taken on the lower plate in the direction of the flow. The y-axis is normal to the plates and the z-axis perpendicular to the xy-plane(see Fig.3.1). The fluid along with the plates are in a rigid body rotation about the y-axis with a uniform angular velocity Ω. A uniform magnetic field of strength B_0 is applied perpendicular to the plates. Since the plates are infinitely long along x and z-axes, all

physical variables, except pressure, depend on y and t only .

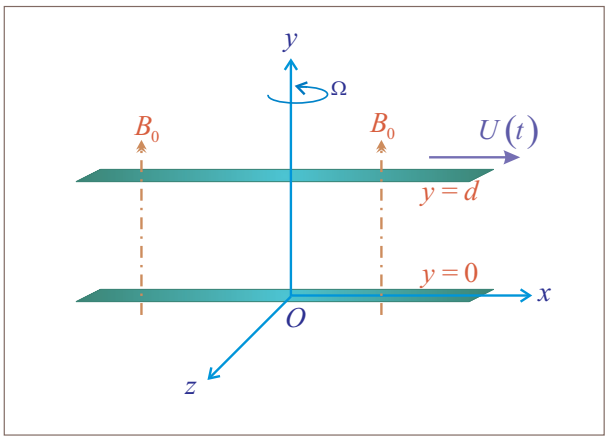

Fig.3.1: *Geometry of the problem*

We shall assume that the induced magnetic field produced by the motion of the conducting fluid is negligible so that $\vec{B} \equiv (0, B_0, 0)$. In the absence of an external electric field the effect of polarisation of the fluid is negligible.We shall also assume that the electric field $\vec{E} = 0$, Meyer [8].

The Navier-Stokes equations of motion for a conducting fluid are

$$\frac{\partial v_x}{\partial t} - 2\Omega v_y = -\frac{1}{\rho}\frac{\partial p}{\partial x} + \nu\frac{\partial^2 v_x}{\partial y^2} - \frac{\sigma B_0^2}{\rho}v_x, \tag{3.1}$$

$$\frac{\partial v_y}{\partial t} + 2\Omega v_x = -\frac{1}{\rho}\frac{\partial p}{\partial y} + \nu\frac{\partial^2 v_y}{\partial y^2} - \frac{\sigma B_0^2}{\rho}v_y, \tag{3.2}$$

$$0 = -\frac{1}{\rho}\frac{\partial p}{\partial z}, \tag{3.3}$$

where ρ, ν, Ω and p are respectively the fluid density, kinematic viscosity, angular velocity and fluid pressure including centrifugal force.
The boundary conditions are

$$v_x = 0 = v_y \text{ at } y = 0 \quad \text{and} \quad v_x = U(t),\ v_y = 0 \text{ at } y = d. \tag{3.4}$$

Under usual boundary layer approximations, equations (3.1) and (3.2) become

$$\frac{\partial v_x}{\partial t} - 2\Omega v_y = \frac{\partial U}{\partial t} + \nu\frac{\partial^2 v_x}{\partial y^2} - \frac{\sigma B_0^2}{\rho}(v_x - U), \tag{3.5}$$

$$\frac{\partial v_y}{\partial t} + 2\Omega(v_x - U) = \nu\frac{\partial^2 v_y}{\partial y^2} - \frac{\sigma B_0^2}{\rho}v_y. \tag{3.6}$$

Introducing non-dimensional variables

$$\eta = \frac{y}{d},\ \ u = \frac{v_x}{U_0},\ \ v = \frac{v_y}{U_0},\ \ U = U_0 f(\tau),\ \ \tau = \frac{\nu t}{d^2} \tag{3.7}$$

equations (3.5) and (3.6) become

$$\frac{\partial u}{\partial \tau} - 2K^2 v = \frac{\partial f}{\partial \tau} + \frac{\partial^2 u}{\partial \eta^2} - M^2(u - f), \tag{3.8}$$

$$\frac{\partial v}{\partial \tau} + 2K^2(u - f) = \frac{\partial^2 v}{\partial \eta^2} - M^2 v, \tag{3.9}$$

where $M^2 = \frac{\sigma\, B_0^2\, d^2}{\rho\nu}$ is the squared-Hartmann number representing the ratio of the electromagnetic (Lorentz) force to the viscous force, $K^2 = \frac{\Omega d^2}{\nu}$ the rotation parameter.
The boundary conditions (3.4) reduce to

$$u = v = 0 \ \text{ at } \ \eta = 0 \quad \text{and} \quad u = f(\tau),\ v = 0 \ \text{ at } \ \eta = 1. \tag{3.10}$$

We assume the plate velocity in the form of a Fourier series as

$$\begin{aligned} f(\tau) &= U_o + \sum_{n=1}^{\infty} [U_n \cos n\omega\tau + {U_n}^* \sin n\omega\tau] \\ &= U_o + \mathbf{Re} \sum_{n=1}^{\infty} \bar{U}_n \exp(in\omega\tau), \end{aligned} \tag{3.11}$$

where $\bar{U}_n = U_n - i{U_n}^*$ and '**Re**' denotes the real part. The coefficients U_0, U_n, ${U_n}^*$ are the dimensionless Fourier constants of the function $f(\tau)$ when expressed in its fundamental period $\frac{2\pi}{\omega}$, where $\omega\left(= \frac{\omega^* d^2}{\nu} \right)$ being the dimensionless frequency of the oscillations. These may be interpreted as dimensionless constants representing the amplitudes of the oscillating plate velocity superposed upon the constant mean velocity U_0.
In view of (3.11), solution of the equations (3.8) and (3.9) can be written in the following form

$$u = u_0(\eta) + \mathbf{Re} \sum_{n=1}^{\infty} u_n(\eta) \exp(in\omega\tau), \tag{3.12}$$

$$v = v_0(\eta) + \mathbf{Re} \sum_{n=1}^{\infty} v_n(\eta) \exp(in\omega\tau). \tag{3.13}$$

On the use of (3.11)-(3.13), equations (3.8) and (3.9) become

$$i\,n\omega u_n - 2K^2 v_n = in\omega \bar{U}_n + {u_n}'' - M^2(u_n - \bar{U}_n), \tag{3.14}$$

$$i\,n\omega v_n + 2K^2(u_n - \bar{U}_n) = {v_n}'' - M^2 v_n, \tag{3.15}$$

where $n = 0, 1, 2, \cdots$.
The boundary conditions (3.10) become

$$u_n = v_n = 0 \ \text{ at } \ \eta = 0 \quad \text{and} \quad u_n = \bar{U}_n,\ v_n = 0 \ \text{ at } \ \eta = 1. \tag{3.16}$$

Equations (3.14) and (3.15) subjected to the boundary conditions (3.16) can easily be solved and the solution for the primary and secondary velocities can be written as

$$\begin{aligned} u(\eta,\tau) &= u_0(\eta) + \mathbf{Re}\sum_{n=1}^{\infty} \bar{U}_n \Big[1 - \frac{1}{2}\{\cosh(\alpha_1 + i\beta_1)\eta + \cosh(\alpha_2 \pm i\beta_2)\eta \\ &- \frac{\cosh(\alpha_1 + i\beta_1)}{\sinh(\alpha_1 + i\beta_1)}\sinh(\alpha_1 + i\beta_1)\eta \\ &- \frac{\cosh(\alpha_2 \pm i\beta_2)}{\sinh(\alpha_2 \pm i\beta_2)}\sinh(\alpha_2 \pm i\beta_2)\eta\Big\}\Big] e^{in\omega\tau}, \end{aligned} \tag{3.17}$$

$$\begin{aligned} v(\eta,\tau) &= v_0(\eta) + \mathbf{Re}\sum_{n=1}^{\infty} \frac{i}{2}\bar{U}_n \big[\cosh(\alpha_1 + i\beta_1)\eta - \cosh(\alpha_2 \pm i\beta_2)\eta \\ &- \frac{\cosh(\alpha_1 + i\beta_1)}{\sinh(\alpha_1 + i\beta_1)}\sinh(\alpha_1 + i\beta_1)\eta \\ &+ \frac{\cosh(\alpha_2 \pm i\beta_2)}{\sinh(\alpha_2 \pm i\beta_2)}\sinh(\alpha_2 \pm i\beta_2)\eta\Big] e^{in\omega\tau}, \end{aligned} \tag{3.18}$$

where the upper sign for $n\omega > 2K^2$ and the lower sign for $n\omega < 2K^2$.
Further, $u_0(\eta)$ and $v_0(\eta)$ are the velocity components corresponding to the steady uniform velocity U_0 and are given by

$$u_0 + iv_0 = U_0\left[1 - \cosh(\alpha + i\beta)\eta + \frac{\cosh(\alpha + i\beta)}{\sinh(\alpha + i\beta)}\sinh(\alpha + i\beta)\eta\right], \tag{3.19}$$

$$\begin{aligned} \text{where} \quad \alpha,\ \beta &= \frac{1}{\sqrt{2}}\left[\left(M^4 + 4K^4\right)^{\frac{1}{2}} \pm M^2\right]^{\frac{1}{2}}, \\ \alpha_1,\ \beta_1 &= \frac{1}{\sqrt{2}}\left[\left\{M^4 + \left(n\omega + 2K^2\right)^2\right\}^{1/2} \pm M^2\right]^{\frac{1}{2}}, \\ \alpha_2,\ \beta_2 &= \frac{1}{\sqrt{2}}\left[\left\{M^4 + \left(n\omega - 2K^2\right)^2\right\}^{\frac{1}{2}} \pm M^2\right]^{\frac{1}{2}}. \end{aligned} \tag{3.20}$$

We shall now discuss a few particular cases of interest:

Case-I: When $n\omega \gg 1$, $K^2 \ll 1$ and $M^2 \ll 1$

When $n\omega$ is large order of magnitude then one can expect boundary layer type flow near the plates. For $n\omega \gg 1$, $K^2 \ll 1$ and $M^2 \ll 1$, the velocity distribution are given by

$$\begin{aligned} u &= u_0(\eta) + \sum_{n=1}^{\infty} \{[U_n \cos n\omega\tau + {U_n}^* \sin n\omega\tau] \\ &- \frac{1}{2}\left[e^{-\alpha_1\eta}\left[U_n \cos(n\omega\tau - \beta_1\eta) + {U_n}^* \sin(n\omega\tau - \beta_1\eta)\right]\right. \\ &+ \left. e^{-\alpha_2\eta}\left[U_n \cos(n\omega\tau - \beta_2\eta) + {U_n}^* \sin(n\omega\tau - \beta_2\eta)\right]\right]\}, \qquad (3.21) \\ v &= v_0(\eta) + \frac{1}{2}\sum_{n=1}^{\infty}\left[e^{-\alpha_1\eta}\left[{U_n}^* \cos(n\omega\tau - \beta_1\eta) - U_n \sin(n\omega\tau - \beta_1\eta)\right]\right. \\ &- \left. e^{-\alpha_2\eta}\left[{U_n}^* \cos(n\omega\tau - \beta_2\eta) - U_n \sin(n\omega\tau - \beta_2\eta)\right]\right], \qquad (3.22) \end{aligned}$$

$$\begin{aligned} \text{where} \quad \alpha_{1,2} &= \left(\frac{n\omega}{2}\right)^{\frac{1}{2}}\left(1 \pm \frac{K^2}{n\omega} + \frac{M^2}{2n\omega}\right), \\ \beta_{1,2} &= \left(\frac{n\omega}{2}\right)^{\frac{1}{2}}\left(1 \pm \frac{K^2}{n\omega} - \frac{M^2}{2n\omega}\right). \qquad (3.23) \end{aligned}$$

Equations (3.21) and (3.22) show the existence of double-deck boundary layers of thicknesses $\mathrm{O}\left\{\left(\frac{n\omega}{2}\right)^{\frac{1}{2}}\left(1 + \frac{K^2}{n\omega} + \frac{M^2}{2n\omega}\right)\right\}^{-1}$ and $\mathrm{O}\left\{\left(\frac{n\omega}{2}\right)^{\frac{1}{2}}\left(1 - \frac{K^2}{n\omega} + \frac{M^2}{2n\omega}\right)\right\}^{-1}$ near the plate $\eta = 0$. These layers may be identified as modified Stokes-Ekman-Hartmann layers as modified by the rotation parameter and magnetic field. It is seen that for each mode of pulsation, i.e. for fixed n, there are two associated layers. The thicknesses of these boundary layers decrease with the increase in n. The boundary layers arising due to higher mode of pulsation ($n > 1$) are confined inside the boundary layer due to fundamental mode of pulsation ($n = 1$). The exponential terms in the above expressions damp out quickly as η increases. When

$$\eta \geq \left(\frac{n\omega}{2}\right)^{\frac{1}{2}}\left(1 \pm \frac{K^2}{n\omega} + \frac{M^2}{2n\omega}\right),$$

$$\begin{aligned} \text{we have,} \quad u &= u_0(\eta) + \sum_{n=1}^{\infty}\left[U_n \cos n\omega\tau + {U_n}^* \sin n\omega\tau\right], \\ v &= v_0(\eta). \qquad (3.24) \end{aligned}$$

The above equations show that for large frequency parameter $n\omega$, the fluctuating part of the primary flow will be in phase with the plate oscillations while the unsteady part of the secondary flow vanishes.

Case-II: When $n\omega \ll 1$, $M^2 \ll 1$ and $K^2 \gg 1$

In this case, the velocity components are given by

$$\begin{aligned} u &= u_0(\eta) + \sum_{n=1}^{\infty} \{[U_n \cos n\omega\tau + {U_n}^* \sin n\omega\tau] \\ &- \frac{1}{2}\left[e^{-\alpha_1\eta}\left[U_n \cos(n\omega\tau - \beta_1\eta) + {U_n}^* \sin(n\omega\tau - \beta_1\eta)\right]\right. \\ &+ \left. e^{-\alpha_2\eta}\ \left[U_n \cos(n\omega\tau + \beta_2\eta) + {U_n}^* \sin(n\omega\tau + \beta_2\eta)\right]\right]\}, \qquad (3.25) \\ v &= v_0(\eta) + \frac{1}{2}\sum_{n=1}^{\infty}\left\{e^{-\alpha_1\eta}\left[{U_n}^* \cos(n\omega\tau - \beta_1\eta) - U_n \sin(n\omega\tau - \beta_1\eta)\right]\right. \\ &- \left. e^{-\alpha_2\eta}\left[{U_n}^* \cos(n\omega\tau + \beta_2\eta) - U_n \sin(n\omega\tau + \beta_2\eta)\right]\right\}, \qquad (3.26) \end{aligned}$$

$$\begin{aligned} \text{where} \quad \alpha_{1,2} &= K\left(1 \pm \frac{n\omega}{4K^2} + \frac{M^2}{4K^2}\right), \\ \beta_{1,2} &= K\left(1 \pm \frac{n\omega}{4K^2} - \frac{M^2}{4K^2}\right). \qquad (3.27) \end{aligned}$$

It is seen from above equations (3.25) and (3.26) that for large rotation, that is for large values of $2K^2$ there exist double-deck boundary layers near the plate $\eta = 0$. The thicknesses of these boundary layers are of order $\mathrm{O}\left\{K\left(1 + \frac{n\omega}{4K^2} + \frac{M^2}{4K^2}\right)\right\}^{-1}$ and $\mathrm{O}\left\{K\left(1 - \frac{n\omega}{4K^2} + \frac{M^2}{4K^2}\right)\right\}^{-1}$ near the plate $\eta = 0$. These layers may be identified as the Ekman layers modified by the frequency $n\omega$ and the Hartmann number M. The exponential terms in the above expressions damp out quickly as η increases. When

$$\eta \geq K\left(1 \pm \frac{n\omega}{4K^2} + \frac{M^2}{4K^2}\right),$$

$$\begin{aligned} \text{we get,} \quad u &= u_0(\eta) + \sum_{n=1}^{\infty}\left[U_n \cos n\omega\tau + {U_n}^* \sin n\omega\tau\right], \\ v &= v_0(\eta). \qquad (3.28) \end{aligned}$$

Similar to the above case-I, it is observed from the above equations that for large rotation parameter K^2, the fluctuating part of the primary flow will be in phase with the plate oscillations while the unsteady part of the secondary flow vanishes.

Case-III: When $M^2 \gg 1$, $K^2 \ll 1$ and $n\omega \ll 1$

In this case also the flow field is of boundary layer type and we obtain the velocity distribution as

$$\begin{aligned} u &= u_0(\eta) + \sum_{n=1}^{\infty} \{[U_n \cos n\omega\tau + U_n^* \sin n\omega\tau] \\ &- \frac{1}{2}\left[e^{-M\eta}\,[U_n \cos(n\omega\tau - \beta_1\eta) + U_n{}^* \sin(n\omega\tau - \beta_1\eta)]\right. \\ &- \left. e^{-M\eta}\ [U_n \cos(n\omega\tau - \beta_2\eta) + U_n^* \sin(n\omega\tau - \beta_2\eta)]]\right\}, \qquad (3.29) \\ v &= v_0(\eta) + \frac{1}{2}\sum_{n=1}^{\infty}\Big\{e^{-M\eta}\,[U_n{}^* \cos(n\omega\tau - \beta_1\eta) - U_n \sin(n\omega\tau - \beta_1\eta)] \\ &- e^{-M\eta}\,[U_n{}^* \cos(n\omega\tau - \beta_2\eta) - U_n \sin(n\omega\tau - \beta_2\eta)]\Big\}, \qquad (3.30) \end{aligned}$$

$$\text{where} \quad \beta_1, \beta_2 = \frac{1}{2M}(n\omega \pm 2K^2).$$

The above expressions show the existence of a single boundary layer of thickness of order of $\mathrm{O}(M)^{-1}$. This layer decreases with increase in M. It is interesting to note that this boundary layer thickness is independent of both $n\omega$ and K^2. It is seen that in certain core $\eta \geq 1/M$, the exponential terms in equation (3.29) and (3.30) damp out and the velocity field reduces to

$$\begin{aligned} u &= u_0(\eta) + \sum_{n=1}^{\infty} [U_n \cos(n\omega\tau) + U_n{}^* \sin(n\omega\tau)], \\ v &= v_0(\eta). \qquad (3.31) \end{aligned}$$

Similar to the above cases-I and -II, in this case also we observed from above equation that for large Hartmann number M, the fluctuating part of the primary flow will be in phase with the plate oscillations while the unsteady part of the secondary flow vanishes.

3.3 Single plate oscillation

In the limit $d \to \infty$, equations (3.18) and (3.19) become

$$\begin{aligned} u &= u_0(\eta) + \sum_{n=1}^{\infty} \{(U_n \cos n\omega^* t + U_n^* \sin n\omega^* t) \\ &- \frac{1}{2}\left(U_n^2 + U_n^{*2}\right)\left[e^{-\frac{\alpha_1{}^* y}{\sqrt{2\nu}}}\left\{\cos\left(n\omega^* t \mp \frac{\beta_1^* y}{\sqrt{2\nu}} - \theta\right)\right\}\right. \\ &+ \left. e^{-\frac{\alpha_2{}^* y}{\sqrt{2\nu}}}\left\{\cos\left(n\omega^* t - \frac{\beta_2{}^* y}{\sqrt{2\nu}} - \theta\right)\right\}\right]\Bigg\}, \qquad (3.32) \\ v &= v_0(\eta) - \sum_{n=1}^{\infty} \frac{1}{2}\left(U_n^2 + U_n^{*2}\right)\left[e^{-\frac{\alpha_1{}^* y}{\sqrt{2\nu}}}\left\{\sin\left(n\omega^* t \mp \frac{\beta_1^* y}{\sqrt{2\nu}} - \theta\right)\right\}\right. \\ &- \left. e^{-\frac{\alpha_2{}^* y}{\sqrt{2\nu}}}\left\{\sin\left(n\omega^* t - \frac{\beta_2^* y}{\sqrt{2\nu}} - \theta\right)\right\}\right], \qquad (3.33) \end{aligned}$$

where $u_0(\eta)$ and $v_0(\eta)$ are the velocity fields corresponding to the steady uniform velocity U_0 and are given by

$$\begin{aligned} u_0(\eta) &= U_0\left[1 - e^{-\frac{\alpha^* y}{\sqrt{2\nu}}}\cos\left(\frac{\beta^* y}{\sqrt{2\nu}}\right)\right], \\ v_0(\eta) &= U_0\, e^{-\frac{\alpha^* y}{\sqrt{2\nu}}}\sin\left(\frac{\beta^* y}{\sqrt{2\nu}}\right), \qquad (3.34) \end{aligned}$$

where

$$\begin{aligned} \theta &= \tan^{-1}\left(U_n^*/U_n\right) \\ \alpha^*, \beta^* &= \left[\left\{\left(\tfrac{\sigma B_0^2}{\rho}\right)^2 + 4\Omega^2\right\}^{\frac{1}{2}} \pm \tfrac{\sigma B_0^2}{\rho}\right]^{\frac{1}{2}}, \\ \alpha_1^*, \beta_1^* &= \left[\left\{\left(\tfrac{\sigma B_0^2}{\rho}\right)^2 + (n\omega^* + 2\Omega)^2\right\}^{\frac{1}{2}} \pm \tfrac{\sigma B_0^2}{\rho}\right]^{\frac{1}{2}}, \qquad (3.35) \\ \alpha_2^*, \beta_2^* &= \left[\left\{\left(\tfrac{\sigma B_0^2}{\rho}\right)^2 + (n\omega^* - 2\Omega)^2\right\}^{\frac{1}{2}} \pm \tfrac{\sigma B_0^2}{\rho}\right]^{\frac{1}{2}}. \end{aligned}$$

The above equations (3.32) and (3.33) represent the velocity components in the presence of a uniform transverse magnetic field in a rotating system when the free-stream velocity oscillates with velocity $U_0 + \sum_{n=1}^{\infty}(U_n \cos n\omega^* t + U_n^* \sin n\omega^* t)$. Equations (3.32) and (3.33) show that the unsteady velocities consists of two parts, one oscillates with amplitude $\frac{1}{2}\left(U_n^2 + U_n^{*2}\right) e^{-\alpha_1^* y/\sqrt{2\nu}}$ and the other with

$\frac{1}{2}\left(U_n^2 + U_n^{*2}\right) e^{-\alpha_2^* y/\sqrt{2\nu}}$ where α_1^* and α_2^* are given by (3.35). The boundary layer corresponding to the amplitude $\frac{1}{2}\left(U_n^2 + U_n^{*2}\right) e^{-\alpha_1^* y/\sqrt{2\nu}}$ at a distance y from the plate oscillates with phase lag of $(\beta_2^* y/\sqrt{2\nu} + \theta)$ for $n\omega^* > 2\Omega$ and phase advance $(\beta_2^* y/\sqrt{2\nu} - \theta)$ for $n\omega^* < 2\Omega$ while the layer corresponding to the amplitude $\frac{1}{2}\left(U_n^2 + U_n^{*2}\right) e^{-\alpha_2^* y/\sqrt{2\nu}}$ oscillates with phase lag of $(\beta_2^* y/\sqrt{2\nu} + \theta)$ either for $n\omega^* > 2\Omega$ or $n\omega^* < 2\Omega$. If $U_n = U_n^* = 0$, then $u(\eta)$ and $v(\eta)$ are given by (3.34). This results are identical with the result obtained by Batchelor [220].

3.4 Flow under harmonic oscillations of the plate

In this section, we shall consider the particular case when the plate velocity is given by

$$f(\tau) \;=\; U_0 + U_1 \cos \omega\tau. \tag{3.36}$$

The flow field is then characterized by

$$\begin{aligned} u(\eta,\tau) &= u_0(\eta) + \mathbf{Re}\Big\{U_1\Big[1 - \frac{1}{2}\{\cosh(\alpha_1 + i\beta_1)\eta + \cosh(\alpha_2 \pm i\beta_2)\eta \\ &- \frac{\cosh(\alpha_1 + i\beta_1)}{\sinh(\alpha_1 + i\beta_1)}\sinh(\alpha_1 + i\beta_1)\eta \\ &- \frac{\cosh(\alpha_2 \pm i\beta_2)}{\sinh(\alpha_2 \pm i\beta_2)}\sinh(\alpha_2 \pm i\beta_2)\eta\Big\}\Big] e^{i\omega\tau}\Big\}, \end{aligned} \tag{3.37}$$

$$\begin{aligned} v(\eta,\tau) &= v_0(\eta) + \mathbf{Re}\Big\{\frac{i}{2}U_1\left[\cosh(\alpha_1 + i\beta_1)\eta - \cosh(\alpha_2 \pm i\beta_2)\eta\right. \\ &- \frac{\cosh(\alpha_1 + i\beta_1)}{\sinh(\alpha_1 + i\beta_1)}\sinh(\alpha_1 + i\beta_1)\eta \\ &+ \left.\frac{\cosh(\alpha_2 \pm i\beta_2)}{\sinh(\alpha_2 \pm i\beta_2)}\sinh(\alpha_2 \pm i\beta_2)\eta\right] e^{i\omega\tau}\Big\}, \end{aligned} \tag{3.38}$$

where α_1, α_2, β_1, β_2 are obtained from (3.20) by putting $n = 1$.

3.5 Results and discussion

In order to observe physical significance of this problem, both the steady and unsteady velocity profiles are depicted graphically against η by employing specific values to various pertinent parameters viz. $M^2 = 5, K^2 = 4, \omega = 12$ and $\omega\tau =$

90^0. Numerical values of shear stresses at $\eta = 0$, amplitude and tangent of phase angles are entered in some Tables.

3.5.1 Primary and secondary velocity profiles

The steady primary velocity u_0 and the secondary velocity v_0 have been drawn against η for different values of K^2 and M^2 in Figs.3.2 and 3.3. It is seen from Fig.3.2 that for fixed M^2, the primary velocity u_0 increases with increase in K^2.

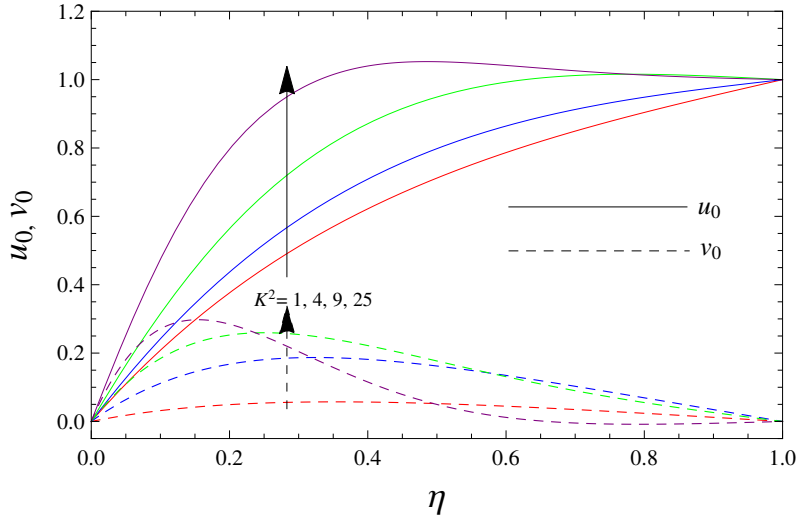

Fig.3.2: *Steady primary velocity u_0 and steady secondary velocity v_0 corresponding to the steady uniform velocity U_0 for K^2 with $M^2 = 5$*

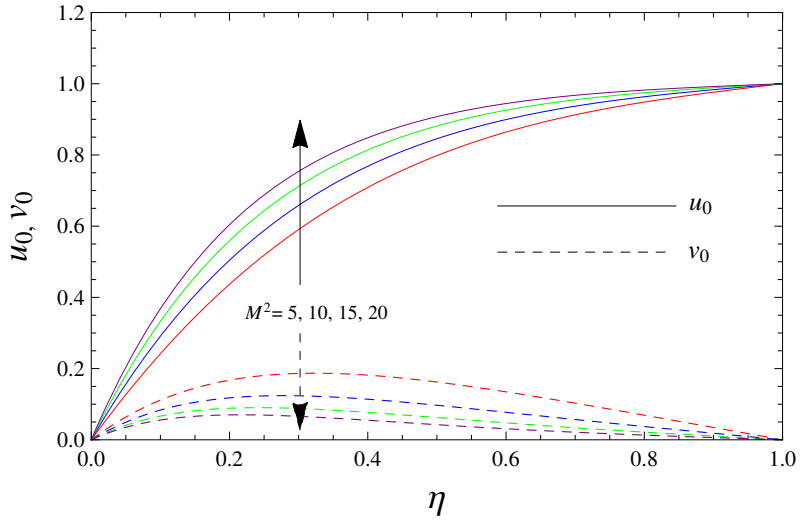

Fig.3.3: *Steady primary velocity u_0 and steady secondary velocity v_0 corresponding to the steady uniform velocity U_0 for M^2 with $K^2 = 4$*

It is also seen that secondary velocity v_0 at any point increases for small values of K^2 while for large values of K^2, it increases near the plate $\eta = 0$ and decreases away form the plate $\eta = 0$. It is seen from Fig.3.3 that the steady primary velocity u_0 increases with increase in M^2 while the steady secondary velocity v_0 decreases with increase in M^2.

For the discussion of the oscillatory part of the flow, the Figures 3.4-3.8 have been drawn against η for the unsteady primary velocity u_{uns} and the secondary velocity v_{uns} for various values of K^2, ω and $\omega\tau$ with $M^2 = 5$ and $U_1 = 1$. It is observed from Fig.3.4 that the unsteady primary velocity at any point increases with increase in rotation parameter K^2. Fig.3.5 shows that for $\omega \geq 2K^2$ the uns-

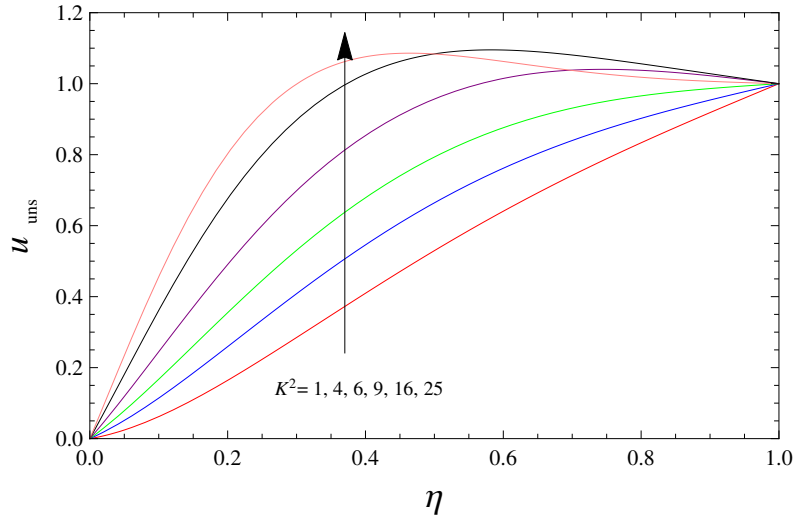

Fig.3.4: *Unsteady primary velocity* u_{uns} *for* K^2 *with* $M^2 = 5$, $\omega = 12$ *and* $\omega\tau = 90^0$

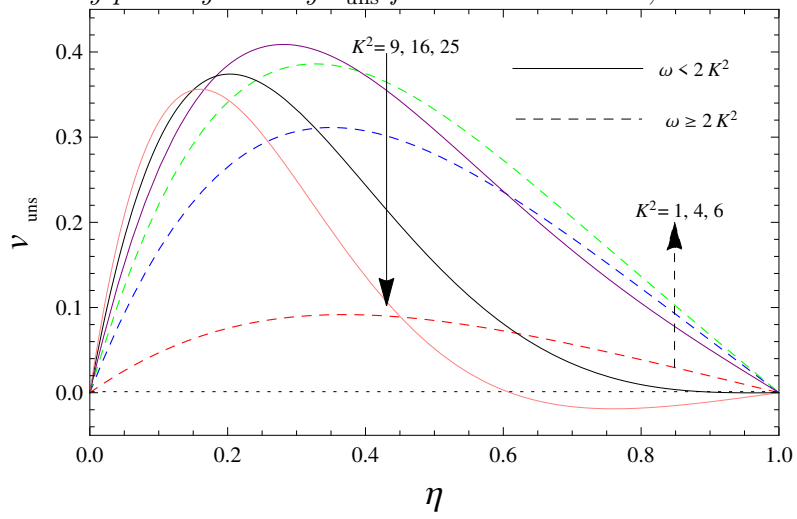

Fig.3.5: *Unsteady secondary velocity* v_{uns} *for* K^2 *with* $M^2 = 5$, $\omega = 12$ *and* $\omega\tau = 90^0$

teady secondary velocity steadily increases while for $\omega < 2K^2$ it increases near the plate $\eta = 0$ and decreases away from the plate $\eta = 0$.

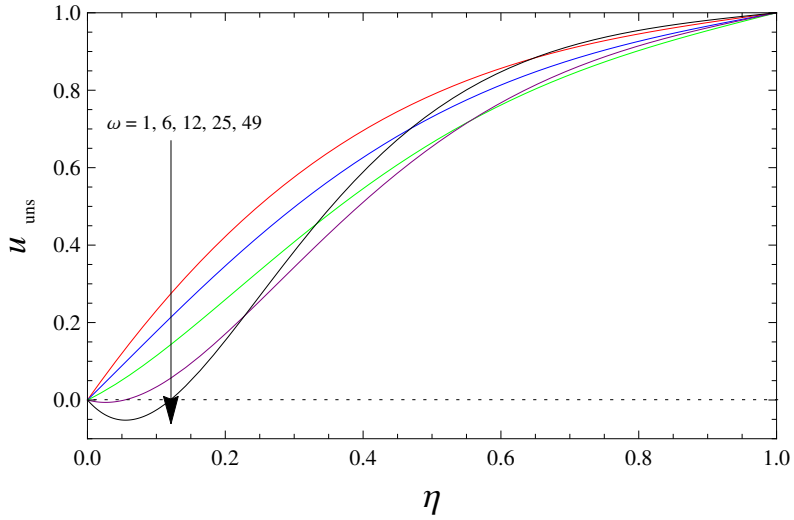

Fig.3.6: *Unsteady primary velocity* u_{uns} *for* ω *with* $M^2 = 5,\ K^2 = 4$ *and* $\omega\tau = 90^0$

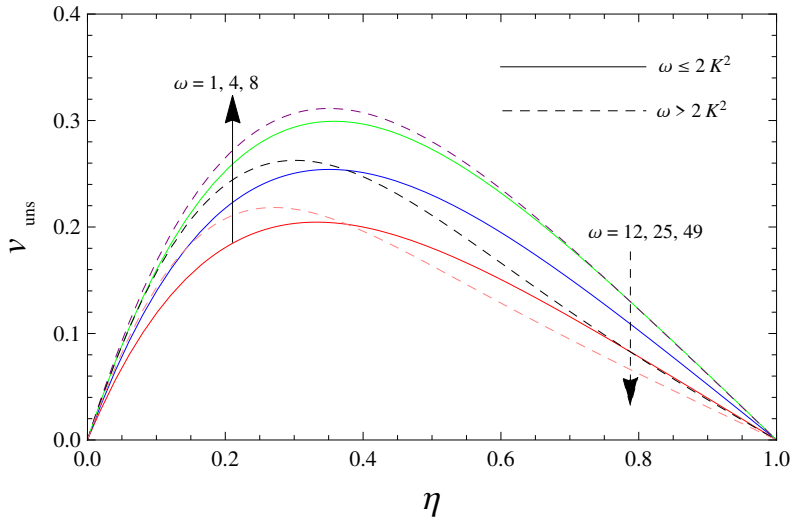

Fig.3.7: *Unsteady secondary velocity* v_{uns} *for* ω *with* $M^2 = 5,\ K^2 = 4$ *and* $\omega\tau = 90^0$

It is seen from Fig.3.6 that for fixed values of M^2, K^2 and $\omega\tau$ the unsteady primary velocity decreases with increase in frequency parameter ω. It is observed from Fig.3.7 that the unsteady secondary velocity increases with increase in ω for $\omega \leq 2K^2$. On the other hand, for $\omega > 2K^2$, it increases near the plate $\eta = 0$ and decreases away from the plate $\eta = 0$. Fig.3.8 shows that the unsteady primary

velocity decreases while the unsteady secondary velocity increases with increase in $\omega\tau$.

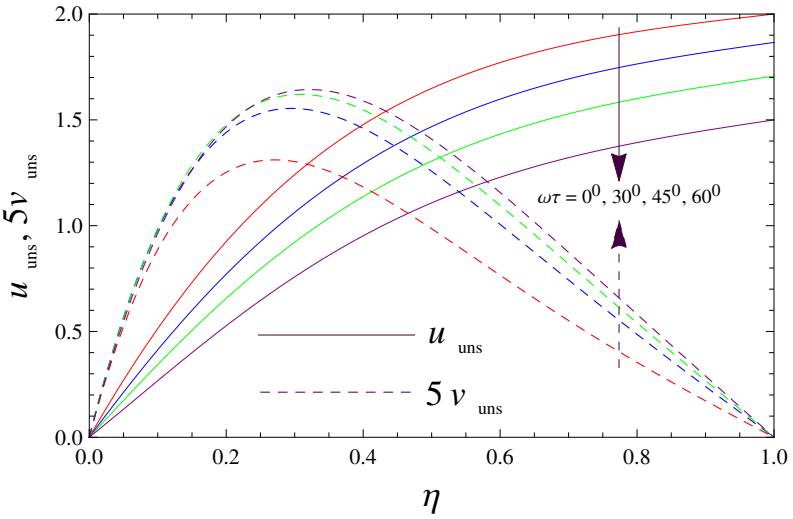

Fig.3.8: *Unsteady velocity distributions* $u_{\rm uns}$ *and* $v_{\rm uns}$ *for* $\omega\tau$ *with* $M^2 = 5$, $\omega = 12$ *and* $K^2 = 4$

3.5.2 Shear stresses

The non-dimensional components of the shear stresses at the plate $\eta = 0$ are given by

$$\begin{aligned} \tau_u &= u_0'(0) + R_1 \cos(\omega t + \phi_1), \\ \tau_v &= v_0'(0) + R_2 \cos(\omega t + \phi_2), \end{aligned} \tag{3.39}$$

where

$$\begin{aligned} u_0'(0) &= \frac{\alpha \sinh 2\alpha + \beta \sin 2\beta}{\cosh 2\alpha - \cos 2\beta}, \qquad v_0'(0) = \frac{\beta \sinh 2\alpha - \alpha \sin 2\beta}{\cosh 2\alpha - \cos 2\beta}, \\ R_1 &= \frac{1}{2}\left[(x_1 + x_2)^2 + (y_1 \pm y_2)^2\right]^{1/2}, \qquad \tan\phi_1 = \frac{y_1 \pm y_2}{x_1 + x_2}, \\ R_2 &= \frac{1}{2}\left[(y_1 \mp y_2)^2 + (x_2 - x_1)^2\right]^{1/2}, \qquad \tan\phi_2 = \frac{x_2 - x_1}{y_1 \mp y_2}, \\ x_1 &= \frac{\alpha_1 \sinh 2\alpha_1 + \beta_1 \sin 2\beta_1}{\cosh 2\alpha_1 - \cos 2\beta_1}, \quad y_1 = \frac{\beta_1 \sinh 2\alpha_1 - \alpha_1 \sin 2\beta_1}{\cosh 2\alpha_1 - \cos 2\beta_1}, \\ x_2 &= \frac{\alpha_2 \sinh 2\alpha_2 + \beta_2 \sin 2\beta_2}{\cosh 2\alpha_2 - \cos 2\beta_2}, \quad y_2 = \frac{\beta_2 \sinh 2\alpha_2 - \alpha_2 \sin 2\beta_2}{\cosh 2\alpha_2 - \cos 2\beta_2}. \end{aligned} \tag{3.40}$$

The values of $u_0'(0)$ and $v_0'(0)$ are given in Table-3.1 for different values of K^2 and M^2. It is observed from Table-3.1 that $u_0'(0)$ increases with an increase in either K^2 or M^2. On the other hand, $v_0'(0)$ increases with an increase in K^2 but it decreases with an increase in M^2.

Table-3.1: *Shear stresses at* $\eta = 0$ *with* $\omega = 9$

	$u_0'(0)$				$v_0'(0)$			
M^2	$K^2 = 1$	$K^2 = 4$	$K^2 = 9$	$K^2 = 16$	$K^2 = 1$	$K^2 = 4$	$K^2 = 9$	$K^2 = 16$
5	2.3163	2.6642	3.8763	4.3255	0.4074	1.4714	2.6243	3.6998
10	3.1875	3.3731	3.5656	4.6661	0.3090	1.1771	2.3041	3.4298
15	3.8845	3.9995	3.0008	5.0175	0.2562	0.9973	2.0539	3.1894
20	4.4788	4.5574	2.5214	5.3731	0.2229	0.8767	1.8585	2.9781

Table-3.2: *Values of amplitude* R_1

	Different values of K^2 with $\omega = 12$					Different values of ω with $K^2 = 6$				
M^2	1	4	6	9	16	1	4	12	16	25
5	3.2172	3.2999	3.4535	3.7957	4.6846	3.1291	3.1967	3.4535	3.6678	4.4000
10	3.7034	3.8331	3.9693	4.2555	5.0633	3.6798	3.7335	3.9693	4.1526	4.6778
15	4.2204	4.3372	4.4550	4.6905	5.3818	4.2066	4.2501	4.4550	4.6064	5.0284
20	4.7157	4.8129	4.9125	5.1082	5.6978	4.7058	4.7407	4.9125	5.0376	5.3888

Table-3.3: *Values of amplitude* R_2

	Different values of K^2 with $\omega = 12$					Different values of ω with $K^2 = 6$				
M^2	1	4	6	9	16	1	4	12	16	25
5	1.0333	1.5221	1.7238	1.9950	2.6026	1.1760	1.3131	1.7238	1.9120	2.0105
10	0.9413	1.3040	1.5131	1.7677	2.2398	0.9131	1.0839	1.5131	1.6849	1.9657
15	0.8305	1.1516	1.3487	1.6014	2.0677	0.7828	0.9452	1.3487	1.5186	1.8394
20	0.7440	1.0387	1.2218	1.4689	1.9418	0.6950	0.8450	1.2218	1.3895	1.7180

The values of amplitudes R_1 and R_2 are entered in Tables-3.2 and -3.3 for various values of K^2, ω and M^2. It is seen from Table-3.2 that R_1 increases with an increase in either M^2 or K^2 or ω. Table-3.3 shows that the amplitude R_2 increases with an increase in either K^2 or ω. On the other hand, for fixed values of K^2 and ω, R_2 decreases with an increase in M^2.

The values of $\tan\phi_1$ and $\tan\phi_2$ have been entered in Tables-3.4 and -3.5 for various values of K^2, ω and M^2. It is seen that $\tan\phi_1$ has a phase lead over the oscillations for $\omega > 2K^2$ and a phase lag over the oscillations for $\omega \leq 2K^2$. It is also seen that $\tan\phi_2$ has always a phase lead over the oscillations either for $\omega > 2K^2$ or $\omega \leq 2K^2$. Tables-3.4 and -3.5 show that the magnitude of $\tan\phi_1$ and $\tan\phi_2$ decreases with an increase in M^2. It is observed from Table-3.4 that the magnitude of $\tan\phi_1$ increases with an increase in ω. Table-3.5 shows that with an increase in K^2, $\tan\phi_2$ increases for $\omega \geq 2K^2$ and decreases for $\omega < 2K^2$.

Table-3.4: *Values of* $\tan\phi_1$

	Different values of K^2 with $\omega = 12$					Different values of ω with $K^2 = 6$				
M^2	1	4	6	9	16	1	4	12	16	25
5	0.4055	0.4680	-0.5181	-0.5224	-0.5400	-0.3175	-0.3895	-0.5181	0.5270	0.5644
10	0.2695	0.3440	-0.3815	-0.4174	-0.4393	-0.2454	-0.2915	-0.3815	0.4094	0.4462
15	0.2015	0.2674	-0.3021	-0.3427	-0.3935	-0.1873	-0.2238	-0.3021	0.3316	0.3761
20	0.1596	0.2164	-0.2486	-0.2886	-0.3493	-0.1489	-0.1794	-0.2486	0.2765	0.3241

Table-3.5: *Values of* $\tan\phi_2$

	Different values of K^2 with $\omega = 12$					Different values of ω with $K^2 = 6$				
M^2	1	4	6	9	16	1	4	12	16	25
5	0.1560	0.4218	0.4910	0.3599	0.2820	0.4844	0.2712	0.4910	0.4944	0.4144
10	0.1146	0.3196	0.3780	0.3016	0.2251	0.0613	0.2021	0.3780	0.3923	0.3469
15	0.0906	0.2519	0.3014	0.2724	0.2058	0.0485	0.1594	0.3014	0.3206	0.3035
20	0.0740	0.2054	0.2481	0.2481	0.1941	0.0397	0.1299	0.2481	0.2686	0.2677

3.6 Conclusion

Consider an unsteady viscous incompressible electrically conducting fluid between two infinite horizontal parallel plates in a rotating system where one of the plate is held at rest and the other oscillates in its own plane. The governing equations are solved assuming the plate velocity in the form of Fourier series. Asymptotic behaviours of the solution are analyzed taking very large values of frequency parameter, rotation parameter and squared-Hartman number. From the above study, the main findings are given below:

- Asymptotic expansion ensures that either for large frequency parameter or for large rotation parameter, there exists a double-deck boundary layers whereas for large Hartmann number there exists a single-deck boundary layer.
- The steady primary velocity increases while the steady secondary velocity decreases with an increase in Hartmann number M.
- The unsteady primary velocity increases with an increase in rotation parameter K^2.
- For large values of K^2 viz. $K^2 > 16$, secondary flow has a back flow near the moving plate.
- Phase angle causes to decrease the unsteady primary velocity while it causes to increase the unsteady secondary velocity.
- The shear stress $u_0'(0)$ increases with an increase in either M^2 or K^2.
- The shear stress $v_0'(0)$ increases with an increase in K^2 while it decreases with an increase in M^2.
- Rotation parameter leads to increase the amplitudes.
- Magnitude of $\tan\phi_1$ and $\tan\phi_2$ decreases with an increase in M^2.